Int. J. Heat Mass Transfer. Vol. 28, No. 10, pp. 1899–1905, 1985
Printed in Great Britain

0017-9310/85 $3.00 + 0.00

Onset of convection in a horizontal porous layer saturated with cold water

DIMOS POULIKAKOS

Department of Mechanical Engineering, University of Illinois at Chicago, P.O. Box 4348, Chicago, IL 60680, U.S.A.

(*Received* 15 *March* 1985 *and in final form* 6 *May* 1985)

Abstract—This paper reports a theoretical investigation on the onset of convection in a horizontal porous layer saturated with water near the vicinity of its density maximum associated with the temperature of 3.98°C at atmospheric pressure. The study aims at determining the critical onset time at which convection starts in the layer, when the temperature of the top wall is suddenly lowered so that the Rayleigh number based on the layer height and the temperature difference between the two horizontal walls is considerably higher than the critical Rayleigh number required to initiate convective instability in the system. The problem was solved via linear stability analysis and by using a time-dependent mean temperature profile. The results reported in this study document the dependence of the critical onset time and the critical wave number on the Rayleigh number R, and the initial temperature of the layer, T_0.

1. INTRODUCTION

THE DETERMINATION of the onset and subsequent development of convective instability in a fluid-saturated porous layer has become a center of attraction in porous media heat transfer and fluid mechanics research in recent years. The counterpart of this problem in classical fluids is the well known 'Bénard problem' which constitutes the main focus of a plethora of studies triggered by the pioneering work of Bénard [1] and Rayleigh [2] in the early 1900s and continuing to the present time. Summaries of the findings of these studies can be found in refs. [3, 4]. The reason behind the 'popularity' of the problem of convective instabilities in a horizontal porous layer is twofold:

(a) It is fundamental in nature, hence, developing a better understanding of this problem may be used as a building block in the investigation of more complicated configurations.
(b) It finds numerous engineering applications exemplified by thermal insulations, geothermal systems, cooling of nuclear reactors and the chemical industry.

When the convective instabilities in the porous medium are driven by thermal buoyancy it is reasonable to expect that the temperature dependence of the density of the fluid saturating the porous medium is of paramount importance. Indeed, in the case of water, the onset of convection as well as the temperature and flow patterns in the layer are affected dramatically by the existence of the density maximum associated with the temperature of 3.98°C at atmospheric pressure. In the vicinity of this density maximum the linear Boussinesq approximation routinely used in natural convection studies is not valid [5–7] and a different temperature–density relation needs to be used.

Relatively few studies have dealt with the phenomenon of natural convection in a porous layer saturated with cold water [8–11]. With reference to the horizontal layer geometry Sun *et al.* [8] and Yen [9] relied on linear stability analysis and experimental measurements, respectively, to define the critical Rayleigh number which marks the onset of convection. Very recently, Blake *et al.* [11] conducted a complete series of numerical experiments to verify the findings in [8, 9] and extend their results to the high Rayleigh number regime. The study in [11] revealed several interesting features with respect to the dependence of the convective pattern (number of cells) and the net heat transfer through the layer on the Rayleigh number, the height-to-length aspect ratio of the system and the bottom wall temperature.

The objective of the present study is to investigate a different aspect of thermal convection in porous media saturated with cold water. Specifically, the present study reports a theoretical (linear stability analysis) investigation of the onset of thermal instabilities in the vicinity of the density maximum at the presence of a *time-dependent* non-linear mean temperature distribution. The system is arranged so that it is unstable in the steady state (at which the mean temperature distribution becomes linear). It is worth noting that the critical values of the Rayleigh number are reported in [8]. Hence, the Rayleigh number values used in this study are purposely higher than the critical values. Since the system is unstable in the steady state, apparently it becomes unstable at some time before steady state is reached. The determination of this critical onset time and its dependence on the various problem parameters is of primary interest in this study. To obtain the onset time, an infinitesimal perturbation is introduced in the system and the evolution of this perturbation in time is observed. If the driving buoyancy mechanism is strong enough to overcome diffusion effects, then, the perturbation is expected to

NOMENCLATURE

A_n Fourier coefficients, equation (15)
B_n Fourier coefficients, equation (15)
c_p specific heat [J kg^{-1} K^{-1}]
F r.m.s. velocity, equation (19)
$\mathbf{g}$ gravitational acceleration vector
G average r.m.s. velocity, equation (18)
H layer height [m]
k effective thermal conductivity [W m^{-1} K^{-1}]
K permeability [m^{-2}]
P pressure [N m^{-2}]
R Darcy-modified Rayleigh number for cold water natural convection, equation (9)
t time [s]
T temperature [°C]
$\bar{T}$ mean temperature [°C]
ΔT temperature difference between the two horizontal walls
u x-component of velocity perturbation [m s^{-1}]
$\mathbf{v}$ velocity vector
v y-component of velocity perturbation [m s^{-1}]
w z-component of velocity perturbation [m s^{-1}]
W velocity function, equation (12)
x, y, z Cartesian coordinates [m].

Greek symbols
α thermal diffusivity [m^2 s^{-1}]
γ constant in density–temperature relationship equation (6) [°C^{-2}]
δ constant in density–temperature relationship equation (6) [°C^{-3}]
η horizontal wave number
θ temperature perturbation
Θ temperature function, equation (12)
λ parameter depending on ΔT, equation (10)
μ viscosity [N s m^{-2}]
ν kinematic viscosity [m^2 s^{-1}]
ρ density [kg m^{-3}]
σ heat capacity ratio, equation (5)
ϕ porosity.

Subscripts
f fluid
r referring to the maximum density
0 pertaining to the initial temperature of the layer
s solid
* dimensionless quantity.

grow in time. In the opposite case, the perturbation will decay in time. The onset time is marked when the perturbation grows to 1000 times its initial value. The value '1000' is of empirical nature, however, numerous investigators [12–17] have used the above method to determine the onset of convection in classical fluids possessing a linear density–temperature dependence and have found good agreement between theoretical predictions and experimental data.

2. MATHEMATICAL FORMULATION

The system of interest is shown schematically in Fig. 1. It consists of a horizontal porous layer saturated with cold water. The onset of convection in the system depends directly upon the initial conditions on temperature. Here, we assume that the system is initially isothermal to T_0 and at $t = 0$, the temperature of the top wall is lowered down to $T_0 - \Delta T$, and is kept at this value thereafter. For the sake of simplicity, the temperature of the cold (top) wall was fixed at 0°C throughout this study. The bottom wall temperature is maintained at its initial value of T_0 at all times. The temperature of 3.98°C associated with the density maximum lies within the region defined by T_0 and $T_0 - \Delta T$, i.e. $T_0 - \Delta T < 3.98°C < T_0$.

The conservation equations for mass, momentum and energy according to the Darcy-homogeneous porous medium model [18, 19] are:

$$\nabla \cdot \mathbf{v} = 0 \tag{1}$$

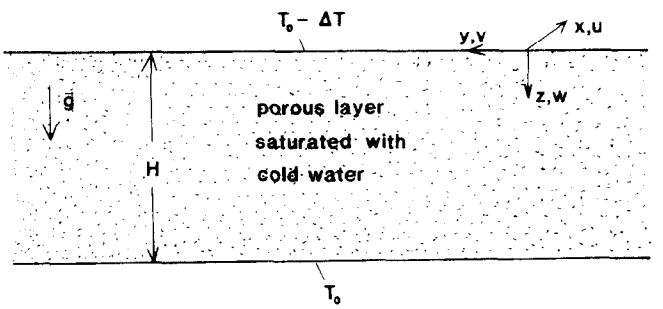

FIG. 1. Schematic of a horizontal porous layer saturated with cold water.

$$\mathbf{v} = \frac{K}{\mu}(-\nabla P + \rho \mathbf{g}) \tag{2}$$

$$\sigma \frac{\partial T}{\partial t} + \mathbf{v}\cdot\nabla T = \alpha \nabla^2 T \tag{3}$$

where $\mathbf{v}$ is the fluid velocity vector ($\mathbf{v} = u\mathbf{i} + v\mathbf{j} + w\mathbf{k}$), $\mathbf{g}$ the gravity vector, P the pressure, T the temperature, ρ the density and t the time. The constants K and μ stand for the permeability of the porous matrix and the fluid viscosity, respectively. Parameter α is the effective thermal diffusivity of the porous medium defined as the ratio of the effective thermal conductivity of the medium k, divided by the fluid thermal capacity $(\rho c_p)_f$. The heat capacity ratio in the energy equation is defined as:

$$\sigma = [\phi(\rho c_p)_f + (1-\phi)(\rho c_p)_s]/(\rho c_p)_f \tag{4}$$

where ϕ is the porosity of the medium and $(\rho c_p)_s$ the thermal capacity of the solid matrix. It is assumed that the fluid and the solid are in local thermal equilibrium.

According to [7–9] the following cubic relation may be used to express the density dependence on temperature in equation (2)

$$\rho = \rho_r[1 - \gamma(T - 3.98°C)^2 - \delta(T - 3.98°C)^3]. \tag{5}$$

This equation was found to be valid in the temperature range 0–30°C. Omitting the cubic term in (6) yields the more familiar parabolic equation valid only in the range 0–8°C [5, 6]. The subscript r in equation (6) stands for the temperature of 3.98°C, $\gamma = 7.94 \times 10^{-6}$ $°C^{-2}$ and $\delta = -6.56 \times 10^{-8}$ $°C^{-3}$.

Due to the peculiar form of the density profile, as the mean temperature distribution evolves in time, two distinct regions can be distinguished in the layer; the potentially unstable region below the point of maximum density and the stable region above this point. In the next section we rely on linear stability analysis to obtain the critical time required by the instabilities originating in the unstable part of the system to give life to convective motions in the layer.

3. STABILITY ANALYSIS

The first step in the stability analysis is to decompose the velocity and the temperature into a mean and a perturbation component. Proceeding as in [3, 4] and omitting the details for brevity, yields the following expressions for the perturbation momentum and energy equations

$$\nabla^2 w_* = -R(\bar{T}_* + \lambda \bar{T}_*^2)\nabla_{2*}^2 \theta_* \tag{6}$$

$$\frac{\partial \theta_*}{\partial t_*} + w_* \frac{\partial \bar{T}_*}{\partial z_*} = \nabla^2 \theta_*. \tag{7}$$

In the above equations the overbar denotes a mean component. Note that since the mean state is stationary the mean velocity field is zero. In addition, the pressure has been eliminated in equation (6). The perturbation equations (6) and (7) have been made dimensionless according to the following definitions:

$$x_*, y_*, z_* = (x, y, z)/H, \quad \bar{T}_* = \frac{\bar{T} - 3.98°C}{\Delta T} \tag{8}$$

$$w_* = w/(\alpha/H), \quad t_* = t/(\sigma H^2/\alpha), \quad \theta_* = \frac{\theta}{\Delta T}.$$

Parameters R (the Rayleigh number for cold water natural convection) and λ are defined as

$$R = \frac{2Kg\gamma(\Delta T)^2 H}{\nu\alpha}, \quad \lambda = \frac{3\delta}{2\gamma}\Delta T. \tag{9, 10}$$

The operator in the RHS of equation (6) stands for

$$\nabla_{2*}^2 = \frac{\partial^2}{\partial x_*^2} + \frac{\partial^2}{\partial y_*^2}.$$

The mean temperature field subject to the conditions of uniform initial temperature (T_0) and fixed boundary temperatures ($\bar{T} = T_0$ along the bottom wall and $\bar{T} = T_0 - \Delta T$ along the top wall) can be obtained by solving the pure conduction equation. The result reads [20]

$$\bar{T}_* = \bar{T}_{*\text{top}} + z_* + \frac{2}{\pi}\sum_{j=1}^{\infty} \sin(j\pi z_*)\frac{e^{-j^2\pi^2 t_*}}{j}. \tag{11}$$

With the mean temperature profile known from equation (11), the perturbation quantities in equations (6) and (7) are assumed to have the form

$$\begin{pmatrix} w_* \\ \theta_* \end{pmatrix} = \begin{pmatrix} W_*(z_*, t_*) \\ \Theta_*(z_*, t_*) \end{pmatrix} \exp[i(\eta_x x_* + \eta_y y_*)] \tag{12}$$

where η_x, η_y are the two components of the horizontal wave number $\eta^2 = \eta_x^2 + \eta_y^2$. Substituting (12) into (6) and (7) yields

$$\frac{\partial^2 W_*}{\partial z_*^2} - \eta^2 W_* = R\eta^2(\bar{T}_* + \lambda \bar{T}_*^2)\Theta_* \tag{13}$$

$$\frac{\partial \Theta_*}{\partial t_*} + W_* \frac{\partial \bar{T}_*}{\partial z_*} = \frac{\partial^2 \Theta_*}{\partial z_*^2} - \eta^2 \Theta_*. \tag{14}$$

The boundary conditions on the velocity perturbation W_* are that the top and bottom walls are shear free (note that the Darcy flow model for porous media does not satisfy the no-slip condition on a solid boundary). The temperature perturbation is assumed to vanish on either boundary ($\Theta_* = 0$ at $z_* = 0, 1$). Based on the above, we seek solutions of equations (13) and (14) in the form of generalized Fourier series with time-dependent coefficients

$$\begin{pmatrix} W_*(z_*, t_*) \\ \Theta_*(z_*, t_*) \end{pmatrix} = \sum_{n=1}^{\infty} \begin{pmatrix} A_n(t_*) \\ B_n(t_*) \end{pmatrix} \sin(n\pi z_*). \tag{15}$$

Combining (13)–(15) and integrating from $z_* = 0$ to 1 yields

$$A_m = -\frac{2R\eta^2}{(m\pi)^2 + \eta^2} \times \int_0^1 \left\{(\bar{T}_* + \lambda \bar{T}_*^2) \sum_{n=1}^{\infty} B_n \sin(n\pi z_*)\sin(m\pi z_*)\right\} dz_* \qquad m, n = 1, 2, 3 \ldots \tag{16}$$

$$\frac{dB_m}{dt_*} = -[(m\pi)^2+\eta^2]B_m - 2\int_0^1 \left\{\frac{\partial \bar{T}_*}{\partial z_*}\sum_{n=1}^{\infty} A_n \sin(n\pi z_*)\sin(m\pi z_*)\right\} dz_* \qquad m,n = 1,2,3.... \quad (17)$$

Equations (16) and (17) can be combined, and then integrated in time. The result of this calculation will determine the evolution of A_m and B_m (hence, the evolution of W_* and Θ_*) with time. The solution method will be outlined briefly in the next section. It is worth noting that the integrals in (16) and (17) cannot be evaluated analytically, hence, they need to be evaluated by numerical integration at each time step. This fact increases the complexity of the problem compared to previous studies on the onset of convection in classical fluids [12–17] possessing a linear density–temperature dependence. In these studies analytical expressions were used to evaluate the likes of the integrals appearing in equations (16) and (17).

4. SOLUTION METHOD

To obtain the numerical solution of equation (17) we need to truncate the Fourier series (15) by keeping only a finite number of terms. Here, the first 20 ($m = n = 20$) terms are retained. Increasing m and n further left the results practically unchanged. In addition, $j = 40$ terms were found to be more than adequate to represent the mean temperature profile, equation (11). Equation (17) was integrated in time by using the fourth-order Runge–Kutta method [21]. The initial condition used for the numerical integration was to set all the Fourier coefficients B_n equal to unity. This type of initial condition is termed in the literature 'the white noise' initial condition. The sensitivity of the solution method on the choice of initial conditions has been discussed in detail in refs. [12, 14, 16]. It appears that using the 'white noise' initial condition yields reasonably good agreement with experimental findings and constitutes the popular choice in investigations of the onset of convection [12–17]. Another point of interest is that of choosing an appropriate time step for the numerical integration. This choice resulted after a trial and error procedure. It was found that smaller time steps were needed for higher values of R. For example, for $T_0 = 10°C$, $R = 10^3$ a time step size equal to 10^{-4} was required while for $T_0 = 10°C$, $R = 1500$ a finer time step size equal to 2.5×10^{-5} was necessary.

Following refs. [12–17] the onset of convection was marked when the average r.m.s. velocity

$$G(t) = \left[\frac{\int_0^1 W_*(z_*,t_*)^2\, dz_*}{\int_0^1 W_*(z_*,0)^2\, dz_*}\right]^{1/2} \quad (18)$$

reached the magnitude of 1000. In addition, the r.m.s. velocity

$$F(z_*,t) = \left[\frac{W_*(z_*,t_*)^2}{\int_0^1 W_*(z_*,0)^2\, dz_*}\right]^{1/2} \quad (19)$$

was used to illustrate the dependence of the fluid motion in the layer on z_*. The above calculations were performed for a sequence of wave numbers while keeping the rest of the parameters fixed. The wave number yielding the minimum onset time was termed critical wave number and the corresponding onset time, critical onset time. Finally, the present study focused on the high Rayleigh number regime since decreasing the Rayleigh number required a very large number of time steps and thus a prohibitive amount of computing time. It is worth clarifying that even though high Rayleigh numbers require fine step sizes as discussed previously, they yield small critical onset times (a manageable number of time steps is needed to yield the critical onset time). Decreasing the Rayleigh number allows for the use of coarser time steps. However, this advantage is offset by the fact that the number of time steps required to mark the onset of convection increases drastically.

5. RESULTS AND DISCUSSION

The dependence of the onset time on the wave number is shown in Fig. 2 for several Rayleigh numbers. The curves reported in Fig. 2 serve to illustrate the 'sharpness' with which the minima (therefore, the critical onset times) are defined. Interestingly,

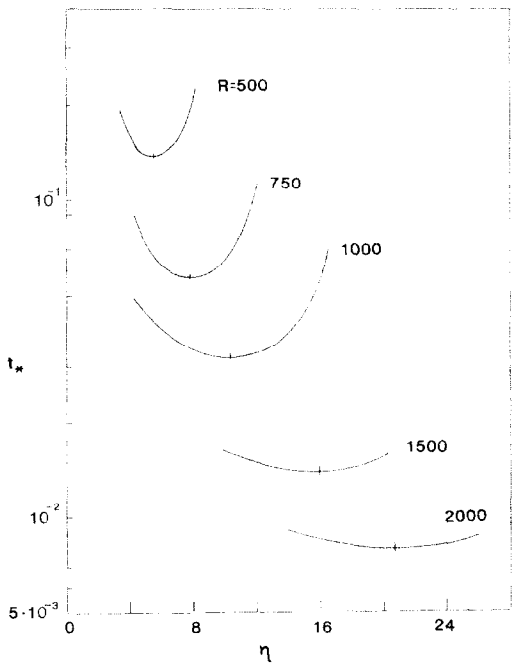

FIG. 2. The dependence of the onset time t_* on the wave number η, for $T_0 = 10°C$.

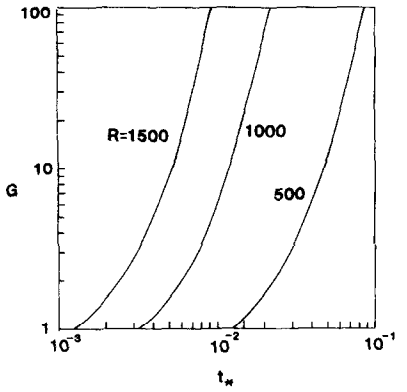

FIG. 3. The growth of the average r.m.s. velocity G for $T_0 = 10°C$. The three curves correspond to the critical wave number of the respective Rayleigh number.

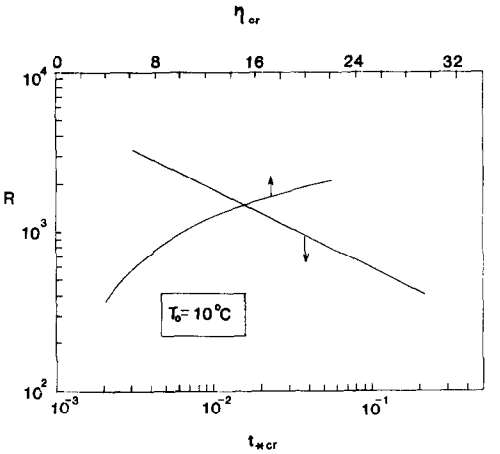

FIG. 5. The dependence of η_{cr} and t_{*cr} on the Rayleigh number for $T_0 = 10°C$.

increasing R yields less sharply defined minima on the t_* vs R curves. The results presented in the remaining figures correspond to critical wave numbers. Figure 3 shows the dependence of the average r.m.s. velocity on time. Clearly, after some time, G grows with t_* in a superexponential manner. This superexponential growth takes place earlier at higher Rayleigh numbers. The vertical profiles for the r.m.s. velocity and the mean temperature at the critical onset time are exemplified via Fig. 4 for two different values of R. Increasing R decreases t_{*cr}. The shape of the curves indicates that at high Rayleigh numbers convection sets in the layer before the cooling effect of the top wall is felt by the bottom wall. Hence, the onset of convection in the finite height layer under examination resembles the onset of convection in a layer of infinite depth. In addition, judging from the location of the density maximum ($\bar{T}_* = 0$) most of the fluid in the layer at t_{*cr} (approx. 85% of the total height for $R = 1000$ and 75% of the total height for $R = 500$) is unstably stratified.

The effect of the Rayleigh number on t_{*cr} and η_{*cr} is illustrated in Fig. 5 for $T_0 = 10°C$. Clearly, t_{*cr} and η_{cr} exhibit opposite dependences on R, that is, increasing R increases η_{cr}, while decreasing t_{*cr} in a linear manner (note the logarithmic coordinate axes in Fig. 5). Based on the definition of the Rayleigh number [equation (9)], if ΔT and H are fixed, increasing R is equivalent to increasing the permeability of the porous medium K (within the limits posed by the validity of the Darcy flow model). In this respect, the results reported in Figs. 2 and 5 quantify the phenomenon of natural convection suppression due to a decrease in the porous medium permeability (K), as one might expect from physical considerations.

Finally, Figs. 6 and 7 depict the dependence of the critical wave number and the critical onset time on the initial temperature of the layer. Increasing T_0 increases η_{cr} and decreases t_{*cr}. It is worth noting, that the

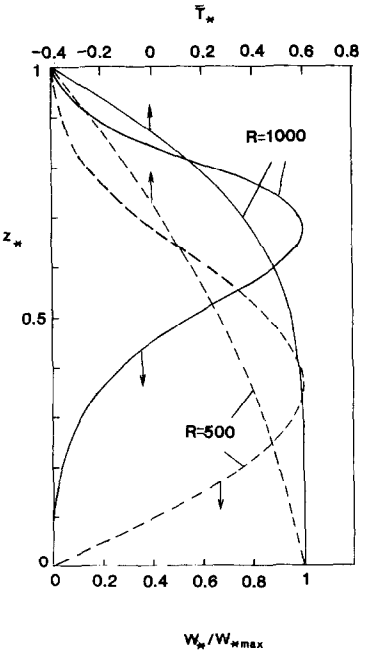

FIG. 4. Distribution in the vertical of the r.m.s. velocity F and mean temperature $\bar{T}_*$ for $T_0 = 10°C$. The curves correspond to the respective critical wave numbers.

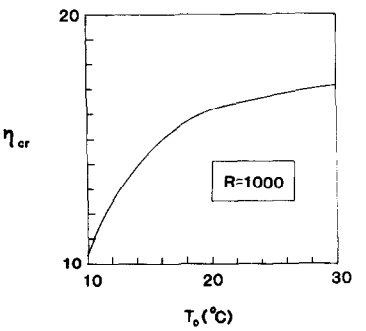

FIG. 6. The effect of T_0 on the critical wave number.

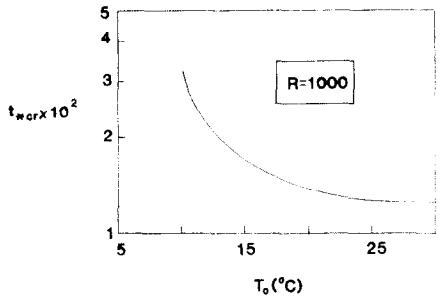

FIG. 7. The effect of T_0 on the critical onset time.

dependence of η_{cr} and t_{*cr} on T_0 is strong for T_0 less than approx. 20°C. For values of T_0 greater than 20°C the critical wave number and the critical onset time exhibit a weak dependence on the initial temperature of the water-saturated porous layer. A physical explanation for this result is speculated as follows: for a layer of fixed height, increasing T_0 while keeping R constant requires a simultaneous decrease in the permeability. It appears that the suppression of natural convection (increase in t_{*crit}), resulting from lowering the permeability, balances out the decrease in t_{*crit}, resulting from increasing T_0, when T_0 becomes greater than approx. 20°C.

6. CONCLUSION

The study reported in this paper relied on linear stability analysis to determine the onset of convection in a porous layer saturated with cold water. The presence of the density extremum of water associated with the temperature of 3.98°C was taken into account by using a cubic temperature density relationship [equation (5)]. The results show that the dimensionless onset time decreases and the critical wave number increases as the Rayleigh number increases. For fixed boundary temperatures and permeability, increasing R is equivalent to increasing the layer depth H. However, since $R \sim H$, $t_* \sim tH^{-2}$ [equation (8)] and from Fig. 5 $t_{*cr} \sim R^{-2}$, then t_{cr}, i.e. the *real* critical onset time is practically independent of H in the high Rayleigh number regime. This result agrees with Foster's findings [12]. The effect of increasing the initial temperature of the layer T_0 is to increase η_{cr} while decreasing t_{*cr}.

The results of this study are in qualitative agreement with reported findings on the onset of convection in classical fluids possessing a linear density–temperature relationship [12–17].

Acknowledgement—Financial support for this research provided by the National Science Foundation under grant No. MEA-8451144 is greatly appreciated.

REFERENCES

1. H. Bénard, Les tourbillons cellulairs dans une nappe liquide transport de la chaleur par convection en regime permanent, *Annls Chim. Phys.* **23,** 62–144 (1901).
2. Lord Rayleigh, On convective currents in a horizontal layer of fluid when the higher temperature is on the underside, *Phil. Mag.* **32,** 529–546 (1916).
3. S. Chandrasekhar, *Hydrodynamic and Hydromagnetic Stability*. Clarendon Press, Oxford (1961).
4. P. G. Drazin and W. H. Reid, *Hydrodynamic Stability*. Cambridge University Press, Cambridge (1981).
5. S. L. Goren, On free convection in water at 4°C, *Chem. Engng Sci.* **21,** 515–518 (1966).
6. D. R. Moore and N. O. Weiss, Non-linear penetrative convection, *J. Fluid Mech.* **61,** 553–581 (1973).
7. Z-S. Sun, C. Tien and Y-C. Yen, Thermal instability of a horizontal layer of liquid with Maximum Density, *A.I.Ch.E. Jl* **15,** 910–915 (1969).
8. Z-S. Sun, C. Tien and Y-C. Yen, Onset of convection in a porous medium containing liquid with a density maximum. *Proc. 4th Int. Heat Transfer Conference*, Paris, Versailles, paper NC 2.11 (1972).
9. Y-C. Yen, Effects of density inversion on free convection heat transfer in a porous layer heated from below, *Int. J. Heat Mass Transfer* **17,** 1349–1356 (1974).
10. J. M. Ramilison and B. Gebhart, Buoyancy induced transport in porous media saturated with pure or saline water at low temperatures, *Int. J. Heat Mass Transfer* **23,** 1521–1530 (1980).
11. K. R. Blake, D. Poulikakos and A. Bejan, Natural convection near 4°C in a water saturated porous layer heated from below, *Int. J. Heat Mass Transfer* **27,** 2355–2364 (1984).
12. T. D. Foster, Stability of a homogeneous fluid cooled uniformly from above, *Phys. Fluids* **8,** 1249–1257 (1965).
13. T. D. Foster, Onset of manifest convection in a layer of fluid with a time depended surface temperature, *Phys. Fluids* **12,** 2482–2487 (1969).
14. E. G. Mahler, R. S. Schechter and E. H. Wissler, Stability of a fluid layer with time-depended density gradients, *Phys. Fluids* **11,** 1901–1912 (1968).
15. M. Kaviany and M. Vogel, Delay in the onset of thermal convection caused by solute gradients, ASME paper No. 84-HT-107 (1984).
16. W. G. Spagenberg and W. R. Rowland, Convective circulation in water induced by evaporative cooling, *Phys. Fluids* **4,** 743–750 (1961).
17. M. Kaviany, Onset of thermal convection in a fluid layer subjected to transient heating from below, *J. Heat Transfer* **106,** 817–823 (1984).
18. M. A. Combarnous, Natural convection in porous media and geothermal systems, *Proc. 6th Int. Heat Transfer Conference*, Vol. 6, pp. 45–59 (1978).
19. P. Cheng, Heat transfer in geothermal systems, *Adv. Heat Transfer* **14,** 1–105 (1979).
20. H. S. Carslaw and J. C. Jager, *Conduction of Heat in Solids*. Oxford, Clarendon Press (1959).
21. J. H. Ferziger, *Numerical Methods for Engineering Applications*. John Wiley, New York (1981).

DEBUT DE LA CONVECTION DANS UNE COUCHE POREUSE HORIZONTALE, SATUREE EN EAU FROIDE

Résumé—On présente une étude théorique sur le début de la convection dans une couche horizontale poreuse saturée d'eau proche du maximum de densité, à la température de 3,98°C et à la pression atmosphérique. Il s'agit de déterminer le temps critique d'apparition de la convection dans la couche lorsque la température de la paroi supérieure est brusquement abaissée de façon que le nombre de Rayleigh basé sur l'épaisseur de la couche et la différence de température entre les deux parois horizontales, soit considérablement plus grand que le nombre de Rayleigh correspondant à l'apparition de l'instabilité du système. Le problème est résolu par l'analyse de la stabilité liénaire et en utilisant un profil de température moyenne dépendant du temps. Les résultats donnés dans cette étude renseignent sur la dépendance du temps critique d'apparition et du nombre d'onde critique vis-à-vis du nombre de Rayleigh R et de la température initiale de la couche, T_0.

DAS EINSETZEN DER KONVEKTION IN EINER WAAGERECHTEN, MIT WASSER GESÄTTIGTEN PORÖSEN SCHICHT

Zusammenfassung—Die Arbeit berichtet über eine theoretische Untersuchung über das Einsetzen von Konvektion in einer waagerechten porösen Schicht, die mit Wasser gestättigt ist. Der Zustand des Wassers ist im Bereich des Dichtemaximums, d.h. bei Atmosphärendruck bei einer Temperatur von 3,98°C. Ziel der Untersuchung ist, den Zeitpunkt zu bestimmen, bei dem in der Schicht Konvektion einsetzt, wenn die Temperatur der Deckelfläche plötzlich abgesenkt wird. Dabei ist die Rayleigh-Zahl, bezogen auf Schichtdicke und Temperaturdifferenz zwischen den beiden waagerechten Begrenzungsflächen erheblich größer als die zum Einsetzen der Konvektion notwendige kritische Rayleigh-Zahl. Das Problem wurde mit Hilfe einer linearen Stabilitätsanalyse und unter Verwendung eines zeitabhängigen mittleren Temperaturverlaufs gelöst. Die Ergebnisse zeigen den Einfluß der Rayleigh-Zahl und der Anfangstemperatur der Schicht T_0 auf die kritische Zeit bis zum Einsetzen der Konvektion und auf die kritische Wellenzahl.

ВОЗНИКНОВЕНИЕ КОНВЕКЦИИ В ГОРИЗОНТАЛЬНОМ ПОРИСТОМ СЛОЕ, НАСЫЩЕННОМ ХОЛОДНОЙ ВОДОЙ

Аннотация—В работе представлены теоретические исследования по возникновению конвекции в горизонтальном пористом слое, насыщенном водой в окрестности максимума плотности, соответствующего температуре 3,98°C при атмосферном давлении. Цель исследования—определение критического времени развития течения в слое, когда температура верхней стенки резко падает до такого уровня, что число Рэлея, основанное на высоте слоя и разности температур между горизонтальными стенками, значительно выше критического числа Рэлея, необходимого для возникновения конвективной неустойчивости в системе. Задача решена с помощью линейного анализа устойчивости и с использованием профиля средней температуры, зависящего от времени. Результаты, представленные в работе, подтверждают зависимость критического времени и критического волнового числа от числа Рэлея R и начальной температуры слоя T_0.